2007 IEEE International Conference on
Robotics and Automation
Roma, Italy, 10-14 April 2007

Posture control of redundant manipulators based on the task oriented stiffness regulation

Koichi Koganezawa

Abstract – **This paper investigates the posture of a manipulator that has redundant DOF similar to human upper extremity. The human arm naturally takes a posture with no wandering although it has some redundant DOF. The authors consider that the posture will be determined task-oriented, which means that human unconsciously takes posture of his/her upper extremities, which is suitable for the task that the endpoint about to do. This study also assumes that all or some joints are capable to adjust the joint stiffness so that the stiffness of the endpoint in the task space is also adjustable. Hence our study aims to establish the way to make the manipulator take a posture that provides a stiffness of the endpoint suitable for the task. The new control formula for shaping the manipulator's posture to provide a desired stiffness of the endpoint is presented followed by the simulation study to verify it.**

Index Terms— ***Posture control, Stiffness, Non-linear elasticity, Stiffness ellipsoid, redundant manipulator***

I. Introduction

It is easily found that some dexterous motions of human articulations owe to the capability of regulating the stiffness in accordance with a task that he/she is about to do. The skeleto-muscular system of human articulations is able to regulate its stiffness mechanically rather than by efferent command from the CNS using exteroceptive force feedback. The key mechanism for regulating the stiffness is the antagonistic structure of the musculo-skeletal system; one agonist and its antagonist muscles counteractively drive one articulation (see Fig.1). Simultaneous stretching of both muscles provides high stiffness of the articulation and both relaxing gives us the low stiffness. It is notified that the non-linear elasticity of muscles is prerequisite for the agonist-antagonistic structure for regulating the stiffness. Some amount of displacement of joint angle requires a respectively small torque at the joint under the equilibrium state of low stretching of both muscles. On the other hand the equilibrium state under high stretching requires a respectively large torque to provide the same amount of angle displacement (see Fig.2). So the stiffness is regulated according to magnitude of stretching of both muscles. It is obvious that linear elasticity does not provide such a stiffness change. A vast amount of physiological studies have elucidated skeletal muscles have the non-linear elasticity like it [1][2][3][4].

Some studies for investigating the stiffness of human arms elucidate that the stiffness ellipse of the arm's endpoint is adjustable in its volume by stretching muscles [5], but its shape is roughly determined according to arm's posture [6].

Some studies in the field of robotics deal with the antagonistic control of joints [7][8][9][10][11][12] and pointed out the importance of the non-linear characteristics of the elastic elements to control the stiffness of the joint [9][10][11], but there have been few papers that propose the control method of stiffness in the practical point of view, although some theoretical approach for stiffness control provides valuable insights[11][13][14].

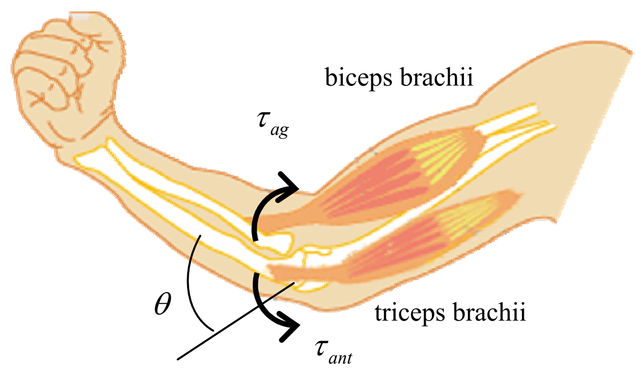

Fig.1 skeleto-muscler system of human elbow joint

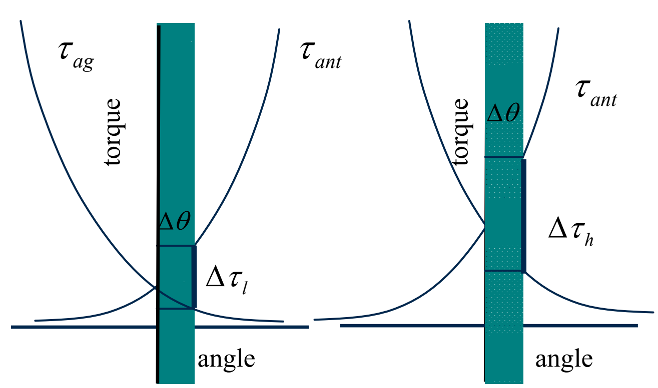

(a) low stretching **(b) high stretching**

Fig.2 Stiffness regulation of antagonistically driven joint

Manuscript received September 15, 2006.

K.Koganezawa is with the Dep. of Mechanical Engineering, Tokai University, Kanagawa, 259-1292, Japan (phone: 0463-58-1211; fax: 0463-59-2207; e-mail:kogane@keyaki.cc.u-tokai.ac.jp).

The aim of this study is to control the stiffness of an anthropomorphic type manipulator's endpoint under some following standpoints:

(i) We assume all or some joints are capable to adjust the joint stiffness independent of adjusting the joint angle. The stiffness of the end point on the task space is composed by linearly mapping the joint stiffness to the task space at the endpoint. So it implies that we assume the stiffness of the endpoint is adjustable.

As briefly introducing in the following section we have developed a new actuator unit called ANLES (actuator with non-linear elastic system) [20-23] that can be used as a sort of voluntary muscle. Therefore we are now progressing the plan to verify the control theory introduced in this paper by using the manipulator that has a musclo-skeletal system for each joint.

(ii) The shape of the *stiffness ellipsoid* that visually shows the magnitude of the stiffness for all of the direction in the task space is roughly determined by the posture of the manipulator.

As noted above the stiffness of the endpoint is a linear mapping of the joint stiffness by the manipulator's Jacobian that is specified by the posture of the manipulator. However the shortage of the DOF of the manipulator confines the mapping domain (we need some extra DOF to specify the stiffness ellipsoid independently to the position and orientation of the endpoint [11]). It implies we have to seek a posture of the manipulator that provides a desired stiffness ellipsoid at the endpoint.

(iii) Human unconsciously takes the posture of his/her upper extremity, which is suitable for the task the endpoint (hand) is about to do. Since the human upper extremity has one or two redundant DOF, it has some freedom to choose a posture even the position of the endpoint is specified. Therefore we also assume an anthropomorphic type manipulator that has one redundant DOF and consider the control method for having the manipulator to take a posture that is suitable for the task in the above-mentioned meaning.

This paper is organized as follows.

In the subsequent section we briefly introduce the actuator unit (ANLES) that we have developed so far. It shows the joint stiffness can be regulated using ANLESes, basically a pair of ANLESes for one DOF in the antagonistic manner.

In the third section we derive the control algorithm for regulating the arm's posture that provides a desired stiffness of the endpoint. The fourth section is devoted to show the simulation analysis. In the last section some conclusive remarks are noted.

II. THE MECHANICAL MODULE FOR THE JOINT ANGLE AND STIFFNESS CONTROL UNDER ANTAGONISTIC DRIVING

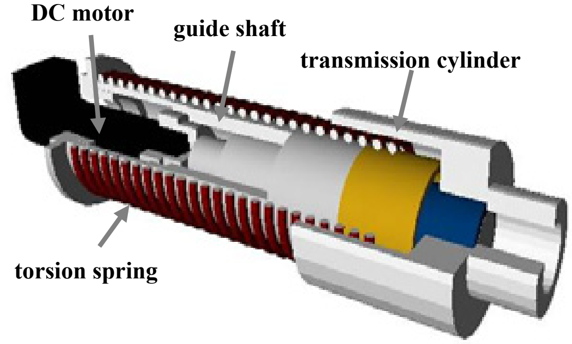

Fig.3 Actuator with non-linear elastic system

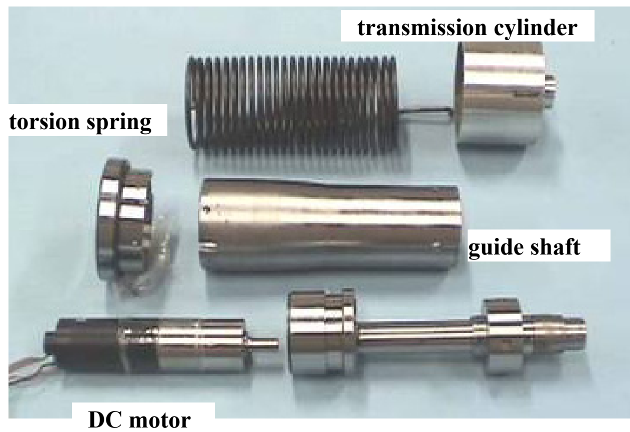

(a) Parts of the fabricated ANLES

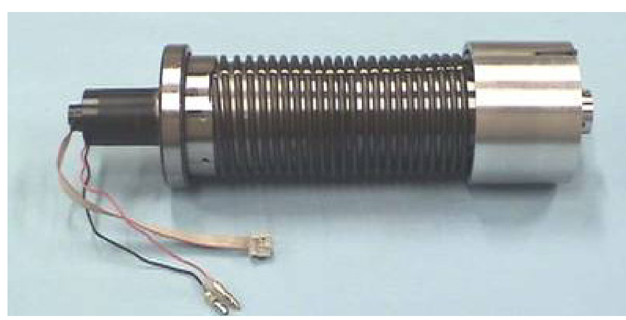

(b) Assembled view of the ANLES

Fig.4 The fabricated ANLES

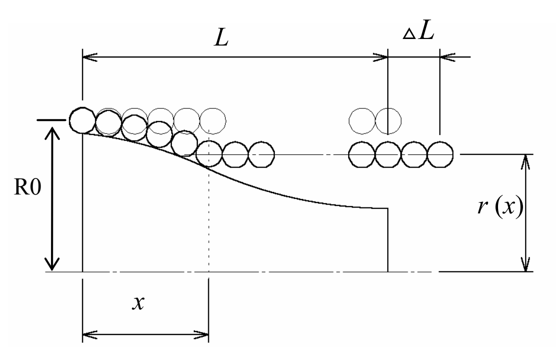

Fig.5 Model of the guide-shaft

In this chapter we briefly introduce the actuator module that can be used as a voluntary muscle, called ANLES (actuator with non-linear elastic system). Fundamentally a pair of ANLESes is used to control a single rotary joint in an antagonistic manner. The details of the design and the development please refer our recent papers [15-18].

A. ANLES (type A)

We have developed the two types of ANLES. The type A is used for controlling a single axis joint, in which a pair of ANLES drives one rotary joint.

Fig.3 shows the structure of the actuator with non-linear elastic system (ANLES) of type A. Fig.4 also shows the parts and the assembled appearance. It consists of DC-motor, guide-shaft, torsion spring, and transmission board (pulley). The torque generated by DC-motor rotates the guide shaft. The guide-shaft rotates the transmission cylinder via the torsion-spring. The transmission cylinder may be combined with a pulley that winds wire. The diameter of the guide shaft smoothly thins down along the rotation axis as schematically shown in Fig.5. The torsion spring covering the guide shaft coils on the surface of the guide shaft from its edge of large radius. The coefficient of the torsion spring at the state that it is coiled by ϕ is calculated by

$$K(\phi) = EI / l_r(\phi) .$$

where, E is the modulus of longitudinal elasticity and I is the second moment of area of the torsion spring wire. $l_r(\phi)$ is the expansion length of the spring wire that actually works as a spring. Now we have a free hand to design the non-linear elasticity through shaping the guide shaft.

B. ANLES (type B)

The ANLES designed for controlling the multi-DOF joint has almost the same structure as the ANLES (type A). The method for designing the guide-shaft to obtain the non-linear elasticity when combined with the torsion spring is identical. But this type of ANLES needs to transform the rotation to the translation, and the vice versa with minimum transmission loss. We therefore employ a super long lead ball screw ($\phi 6$ diameter of the rod with 6 mm lead) embedded into the guide-shaft as shown in Fig.6 and located the DC-motor outside the guide-shaft.

C. Single DOF joint controlled by two ANLESes (type B) and stiffness regulation

Fig.7 shows the single DOF joint. It was built as an intermediate stage aiming to construct a three DOF joint similar to a wrist joint. So that it is controlled by two tendons, in each of which the ANLES(type (B)) shown in Fig.6 is equipped. The DC motor embedded under the base plate rotates the ball screw rod via the universal joint. If the DC motors of both ANLESes rotate the same torsion angle with the identical direction, the same amount of torque is generated

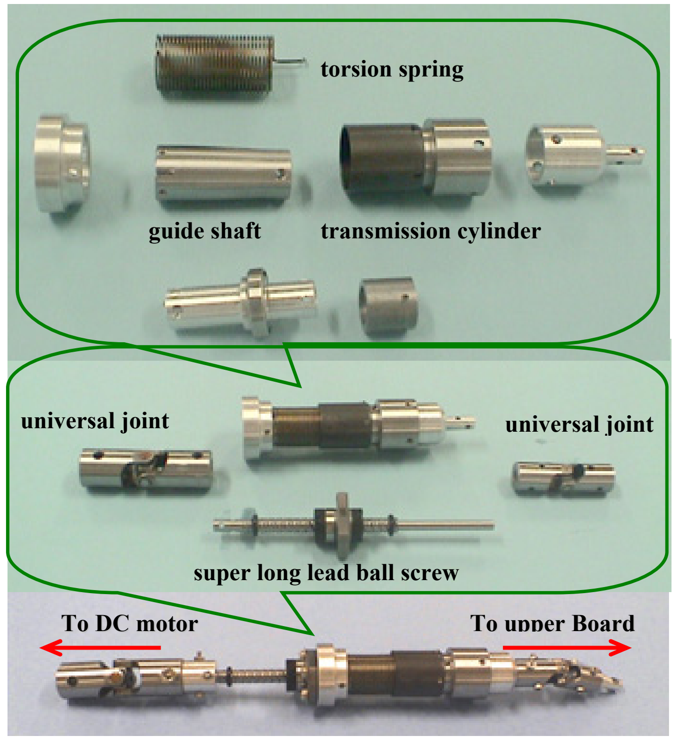

Fig.6 ANLES designed for controlling multi-DOF joint

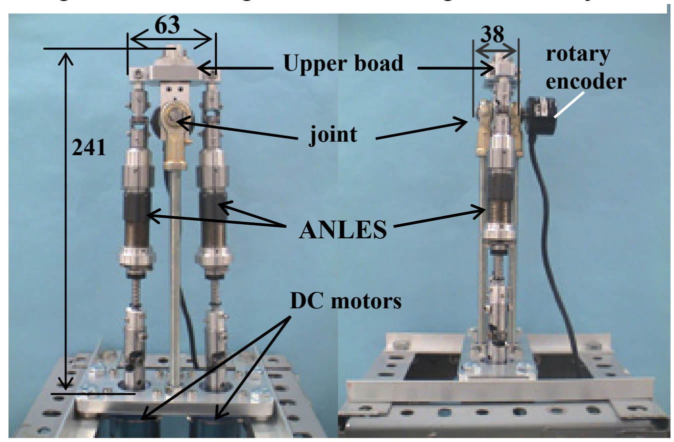

Fig.7 Single DOF ADJ (type B) controlled by two ANLESes

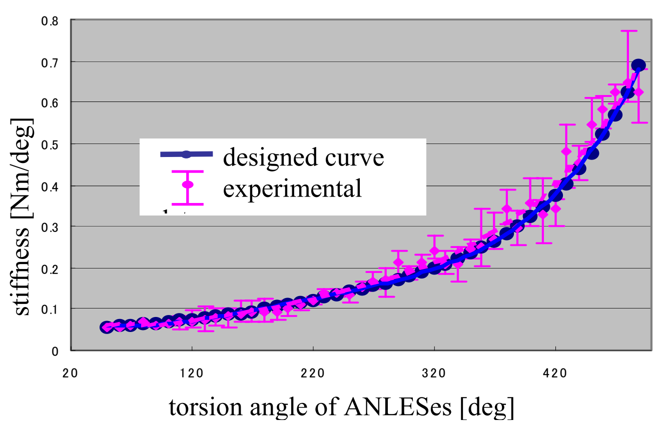

Fig.8 Stiffness of the ADJ (type(B)) shown in Fig.7 controlled by the torsion angle of the ANLESes

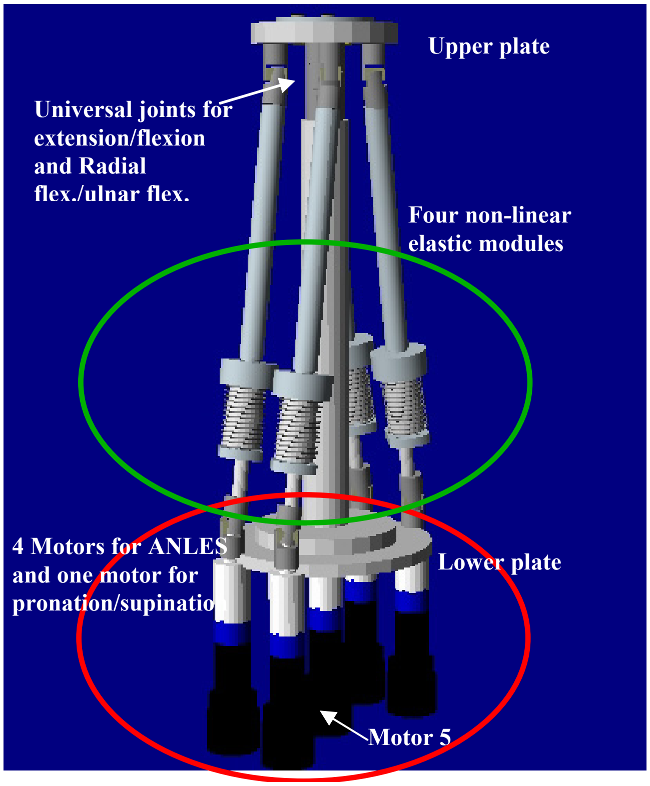

Fig.9 Structure of the three DOF wrist joint using 4 ANLESes

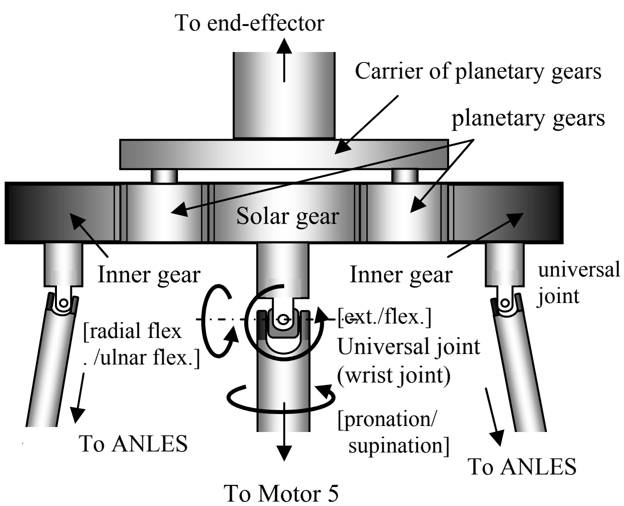

Fig.10 The structure of the upper plate

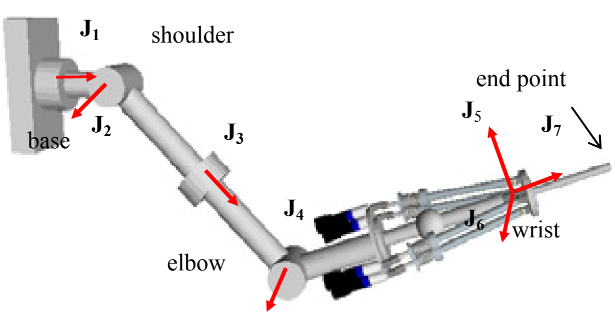

Fig.11 Model of seven D.O.F manipulator equipped with the mechanism shown in Fig.9

and it is transformed to the same amount of traction force by the super-lead ball screws.

These two forces work as torques about the rotary joint, the same amplitude but opposite direction, so that they are *antagonistically* cancelled and the rotary joint will not rotate. In this case the DC motor purely twists the torsion spring of the ANLES, which enhances the stiffness of the rotary joint with no rotation. If the balance of the traction forces of two rods breaks the joint rotates to reach the equilibrium state that is determined not only by the traction forces but also by the moment arms between the axis of the rotary joint and each rods, which is varied by the angle of the rotary joint.

Fig.8 shows the experimental results and the theoretical curve of the stiffness of the joint shown in Fig.7 when both of the ANLESes twist the same amount of torsion angle. The error bar shows the variations of the measured data of five trials. As shown in Fig.8, the experimental data are well congruent with the designed stiffness curve.

D. Three DOF joint controlled by multiple ANLESes

We are now constructing the wrist joint having three DOF. As shown in Fig.9 four ANLESes of type B (just identical to the one shown in Fig.6) are used for controlling two DOF (the extension/flexion and the radial flexion/ulnar flexion). The remaining one DOF is controlled by one motor (motor 5 in Fig.9). This design is determined in the practical point of view since it is very hard in terms of the capacity and the disposition to equip the extra two ANLES for controlling the pronation/spination. Alternatively we equip a planetary gear system into the upper plate as shown in Fig.10. The motor 5 rotates the solar gear providing the rotation of the carrier of the planetary gears. It is an active pronation/spination. On the other hand an external torque loaded on the end point rotates the carrier, which leads the rotation of the inner gear and the twist of four ANLESes. Therefore it enables some elastic rotation of pronation/spination although its stiffness cannot independently be specified. It depends on the torsion angles of four ANLESes.

III. The Theory of Posture Control for Obtaining the Ideal Stiffness of the Endpoint

In this section we derive the formula to provide the posture of the anthropomorphic manipulator. The assumed model has one or more redundant DOF as shown in Fig.11. Our study has one standpoint that the DOF of the shoulder and the elbow, total four in the model of Fig.11, are used to determine the position of the wrist and the direction of the forearm, which roughly specifies the stiffness matrix of the endpoint. The precise adjustment of the stiffness matrix is then achieved by the three DOF of the wrist joint. So as a first step of our study we assume to equip the mechanism shown in Fig.9 as an actuator for the wrist joint and also assume to equip single rotary joints driven by high-geared motors for the other DOF existing at the shoulder and the elbow. As a

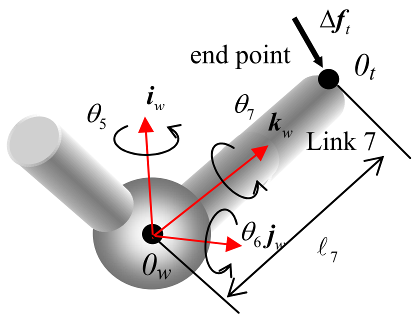

Fig.12 Wrist joint coordinate and the end point

second step we are planning to equip a pair of ANLESes of type A (Fig.3) to all of the DOF at the shoulder and the elbow.

Let us set the wrist coordinate as shown in Fig.12, in which the unit vector $\boldsymbol{k}_w$ is assumed to be in parallel to $\overrightarrow{O_wO_t}$. Let us suppose some variance of external force vector $\Delta\boldsymbol{f}_t^{(w)}=[\Delta f_{ti}\ \Delta f_{tj}]^T$ is loaded at the end point. It gives rise to the variance of the torque vector $\Delta\boldsymbol{\tau}_w^{(w)}=[\Delta\tau_{wi}\ \Delta\tau_{wj}]^T$ at the origin of the wrist coordinate,

$$\Delta\boldsymbol{\tau}_w^{(w)}=l_7\boldsymbol{C}\,\Delta\boldsymbol{f}_t^{(w)},\quad \text{with } \boldsymbol{C}\equiv\begin{bmatrix}0 & -1\\ 1 & 0\end{bmatrix} \tag{1}$$

where, the superscript "(*)" designates the coordinate system. The rotational stiffness matrix $\left(\overline{S_w^R}\right)^{(w)}\in\Re^{2\times2}$ can be defined as the relation between $\Delta\boldsymbol{\tau}_w^{(w)}$ and the variance of the rotation about $\boldsymbol{i}_w$ and $\boldsymbol{j}_w$; $\Delta\boldsymbol{\theta}_w=[\Delta\theta_5\ \Delta\theta_6]^T$,

$$\Delta\boldsymbol{\tau}_w=-\left(\overline{\boldsymbol{S}_w^R}\right)^{(w)}\Delta\boldsymbol{\theta}_w \tag{2}$$

The corresponding linear stiffness matrix at the end point is calculated by,

$$\left(\overline{\boldsymbol{S}_t^L}\right)^{(w)}=\left(1/l_7^2\right)\boldsymbol{C}^{\mathrm{T}}\left(\overline{\boldsymbol{S}_w^R}\right)^{(w)}\boldsymbol{C}\in\Re^{2\times2} \tag{3}$$

Now we expand the 2×2 matrix $\left(\overline{\boldsymbol{S}_t^L}\right)^{(w)}$ to the 3×3 matrix by introducing the sufficiently large constant α,

$$\left(\boldsymbol{S}_t^L\right)^{(w)}=diag\left\{\left(\overline{\boldsymbol{S}_t^L}\right)^{(w)},\alpha\right\} \tag{4}$$

α is the linear stiffness along $\boldsymbol{k}_w$, hence it will be considered as the modulus of longitudinal elasticity of the link 7. $\left(\boldsymbol{S}_t^L\right)^{(w)}$ can be transformed into the expression on the task space (inertia) coordinate by using the rotation matrix of the wrist coordinate: $\boldsymbol{R}_{0w}$

$$\boldsymbol{S}_t^L=\boldsymbol{R}_{0w}\left(\boldsymbol{S}_t^L\right)^{(w)}\boldsymbol{R}_{ow}^T \tag{5}$$

Now let us denote the ideal linear stiffness matrix on the task space by $\tilde{\boldsymbol{S}}_t^L\in\Re^{3\times3}$ and also let us denote the rotation matrix from the current stiffness matrix $\boldsymbol{S}_t^L$ to the ideal one by $\boldsymbol{R}_s$. It follows,

$$\boldsymbol{S}_t^L=\boldsymbol{R}_s^{\mathrm{T}}\tilde{\boldsymbol{S}}_t^L\boldsymbol{R}_s \tag{6}$$

$\boldsymbol{R}_s$ can be expressed by using the unit vector of the rotation axis $\boldsymbol{v}_s=[v_{sx}\ v_{sy}\ v_{sz}]^T$ and the rotation angle $\Delta\phi_s$ as,

$$\boldsymbol{R}_s=\boldsymbol{I}+\hat{\boldsymbol{v}}_s\sin\left(\Delta\phi_s\right)+\left(1-\cos\left(\Delta\phi_s\right)\right)\hat{\boldsymbol{v}}_s^2 \tag{7}$$

where, $\hat{\boldsymbol{v}}_s$ stands for the skew-symmetric matrix that comprises the elements of the vector $\boldsymbol{v}_s$ such as,

$$\hat{\boldsymbol{v}}_s=\begin{bmatrix}0 & -v_s^z & v_s^y\\ v_s^z & 0 & -v_s^x\\ -v_s^y & v_s^x & 0\end{bmatrix}$$

Let us assume $\Delta\phi_s$ is so small that (7) can be simplified as,

$$\boldsymbol{R}_s\cong\boldsymbol{I}+\hat{\boldsymbol{v}}_s\sin\left(\Delta\phi_s\right) \tag{8}$$

It follows by substituting (8) into (5),

$$\begin{aligned}\boldsymbol{S}_t^L&=\left(\boldsymbol{I}+\hat{\boldsymbol{v}}_s\Delta\phi_s\right)^{\mathrm{T}}\tilde{\boldsymbol{S}}_t^L\left(\boldsymbol{I}+\hat{\boldsymbol{v}}_s\Delta\phi_s\right)\\ &=\left(\boldsymbol{I}-\hat{\boldsymbol{v}}_s\Delta\phi_s\right)\tilde{\boldsymbol{S}}_t^L\left(\boldsymbol{I}+\hat{\boldsymbol{v}}_s\Delta\phi_s\right)\\ &=\tilde{\boldsymbol{S}}_t^L+\left(\tilde{\boldsymbol{S}}_t^L\hat{\boldsymbol{v}}_s-\hat{\boldsymbol{v}}_s\tilde{\boldsymbol{S}}_t^L\right)\Delta\phi_s-\hat{\boldsymbol{v}}_s\tilde{\boldsymbol{S}}_t^L\hat{\boldsymbol{v}}_s\left(\Delta\phi_s\right)^2\end{aligned}$$

By neglecting again the third term of the right hand side due to the assumption of $\Delta\phi_s$ being so small, we have,

$$\Delta\boldsymbol{S}_t^L\cong\left(\tilde{\boldsymbol{S}}_t^L\hat{\boldsymbol{v}}_s-\hat{\boldsymbol{v}}_s\tilde{\boldsymbol{S}}_t^L\right)\Delta\phi_s,\quad \text{with }\ \Delta\boldsymbol{S}_t^L\equiv\boldsymbol{S}_t^L-\tilde{\boldsymbol{S}}_t^L \tag{9}$$

We can derive $\boldsymbol{v}_s\Delta\phi_s$ from the relation (9). It is not necessary to calculate $\Delta\phi_s$ although it is capable since $|\boldsymbol{v}_s|=1$.

$\boldsymbol{v}_s\Delta\phi_s$ should be come about the variation of the joint angles residing at the shoulder and the elbow. Let us denote it as $\Delta\boldsymbol{\theta}_{se}$ (= $[\Delta\theta_1\ \Delta\theta_2\ \Delta\theta_3\ \Delta\theta_4]^T$ if we consider an anthropomorphic type manipulator as shown in Fig.11). It follows by introducing the Jacobian matrix of the wrist joint coordinate $\boldsymbol{J}_{ow}$,

$$\begin{bmatrix}\boldsymbol{v}_s\Delta\phi_s\\ \boldsymbol{0}_3\end{bmatrix}=\boldsymbol{J}_{ow}\Delta\boldsymbol{\theta}_{se} \tag{10}$$

Dividing the $\boldsymbol{J}_{ow}$ into the rotation part (the upper three rows) and the linear part (the lower three rows) such as $\boldsymbol{J}_{ow}=\left[\left(\boldsymbol{J}_{ow}^R\right)^T\ \left(\boldsymbol{J}_{ow}^L\right)^T\right]^T$, we have,

$$\boldsymbol{v}_s\Delta\phi_s=\boldsymbol{J}_{ow}^R\Delta\boldsymbol{\theta}_{se} \tag{11}$$

$$\boldsymbol{0}_3=\boldsymbol{J}_{ow}^L\Delta\boldsymbol{\theta}_{se} \tag{12}$$

The general solution of (11) with respect to $\Delta\boldsymbol{\theta}_{se}$ is,

$$\Delta\boldsymbol{\theta}_{se}=\left(\boldsymbol{J}_{ow}^R\right)^{\dagger}\boldsymbol{v}_s\Delta\phi_s+\mathrm{P}^{\perp}\left(\boldsymbol{J}_{ow}^R\right)\boldsymbol{\eta} \tag{13}$$

where, $(*)^{\dagger}$ designates the generalized inverse of the matrix "*" and $P^{\perp}(*)$ is the null- projection operator that projects the vector into the complementary space defined by the matrix "*". $\boldsymbol{\eta}$ is an arbitrary vector.

It follows by substituting (13) into (12),

$$\boldsymbol{J}_{ow}^L\left[\left(\boldsymbol{J}_{ow}^R\right)^{\dagger}\boldsymbol{v}_s\Delta\phi_s+\mathrm{P}^{\perp}\left(\boldsymbol{J}_{ow}^R\right)\boldsymbol{\eta}\right]=\boldsymbol{0}_3$$

Solving it with respect to $\boldsymbol{\eta}$ and substituting into (13) we have the final result by utilizing the nilpotent property of the projection operator,

$$\Delta\boldsymbol{\theta}_{se}=\left[\boldsymbol{I}-\mathrm{P}^{\perp}\left(\boldsymbol{J}_{ow}^{R}\right)\left(\boldsymbol{J}_{ow}^{L}\right)^{\mathrm{T}}\left(\boldsymbol{J}_{ow}^{L}\mathrm{P}^{\perp}\left(\boldsymbol{J}_{ow}^{R}\right)\left(\boldsymbol{J}_{ow}^{L}\right)^{\mathrm{T}}\right)^{-1}\boldsymbol{J}_{ow}^{L}\right]\left(\boldsymbol{J}_{ow}^{R}\right)^{\dagger}\boldsymbol{v}_s\Delta\phi_s \tag{14}$$

The part of the square bracket in (14) can be viewed as the *weighted projection operator* that projects the vector into the complementary space of $\boldsymbol{J}_{ow}^{L}$ under the weight matrix $\mathrm{P}^{\perp}\left(\boldsymbol{J}_{ow}^{R}\right)$ so that (14) can be written as,

$$\Delta\boldsymbol{\theta}_{se}=\mathrm{P}^{\perp}_{\mathrm{P}^{\perp}\left(\boldsymbol{J}_{ow}^{R}\right)}\left(\boldsymbol{J}_{ow}^{L}\right)\left(\boldsymbol{J}_{ow}^{R}\right)^{\dagger}\boldsymbol{v}_s\Delta\phi_s \tag{15}$$

[Remark 1] The inverse operation in (14) may fail because of $\mathrm{P}^{\perp}\left(\boldsymbol{J}_{ow}^{R}\right)$ being a rank deficient. It is due to a shortage of DOF at the shoulder and the elbow. In this case the following equation in lie of (14) offers fairly good results,

$$\Delta\boldsymbol{\theta}_{se}=\left[\boldsymbol{I}-\mathrm{P}^{\perp}\left(\boldsymbol{J}_{ow}^{R}\right)\left(\boldsymbol{J}_{ow}^{L}\right)^{\mathrm{T}}\left(\boldsymbol{J}_{ow}^{L}\left(\boldsymbol{J}_{ow}^{L}\right)^{\mathrm{T}}\right)^{-1}\boldsymbol{J}_{ow}^{L}\right]\left(\boldsymbol{J}_{ow}^{R}\right)^{\dagger}\boldsymbol{v}_s\Delta\phi_s \tag{16}$$

although (16) does not assure to hold the position of the wrist origin, which is the identical meaning that (12) is not held.

[Remark 2] As found in the derivation of (14) it requires small rotation of $\boldsymbol{v}_s\Delta\phi_s$ ((8)(9)) so that (14) should be calculated successively by assigning the small value for $\boldsymbol{v}_s\Delta\phi_s$.

IV. The simulation

Fig.13 shows the configuration of the seven DOF manipulator served on the simulation study. It is supposed that the suspension spring or the actuator compensates the gravitational torque loaded on each joint individually. The task for the manipulator is to draw the sliding door as shown I Fig.14. It is postulated that posture like the left figure is unnatural for the task and it should be changed to the one like the right figure. The rotation angle $\Delta\phi_s$ is divided by 1000 and (14) or (16) are calculated 1000 times to reach the desired posture.

Table 1 Simulation results

Joint angle [rad]	θ_1	θ_2	θ_3	θ_4	θ_5	θ_6	θ_7
Initial	-0.6	0.55	-1.8	2.5	0.2	0.25	0.0
Desired	-0.8	0.027	-1.1	2.5	0.2	0.25	0.0
After rotation	-0.494	0.049	-1.463	2.515	0.2	0.25	0.0
Error	0.306	0.029	0.363	0.015	0.0	0.0	0.0

The result of the calculation is summarized in Table 1. In this case all of the computations are carried out based on (16).

Fig.15 shows the stiffness ellipsoid of the end-point, which are directly calculated from the stiffness matrix. As shown the posture regulation provides the stiffness ellipsoid that is almost identical shape to the desired one. Fig.16 shows the postures of the manipulator. The regulated posture is fairly

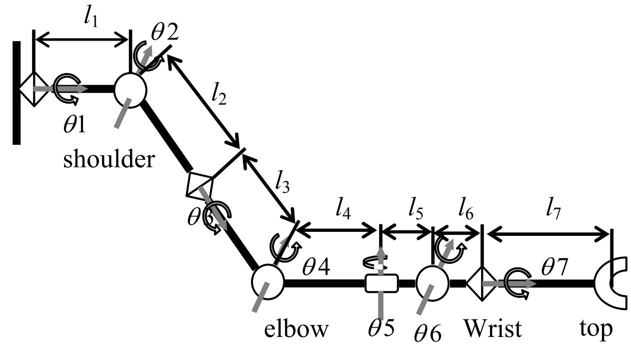

Fig.13 The simulation model of seven DOF manipulator and its link length

a) Unnatural posture b) Natural posture

Fig.14 Posture to open the sliding door

close to the desired one. But as found in Table 1 some small discrepancies exist, the reason of which is considered for using (16) in lieu of (14) for avoiding ill-conditioned computation. However As shown in Table 2 the wrist joint stays the initial position satisfactory.

Table 2 The position of the wrist joint

	X [m]	**Y** [m]	**Z** [m]
Initial Position	-0.0859	0.0293	0.1287
After regulation	-0.0834	0.0298	0.1270
Error	0.0025	0.0005	0.0017

V. Conclusions

This paper proposes a method for determining the posture of the redundant manipulator on the task bases. It stands on one postulation that the human takes his/her posture of the upper extremities, which provides a stiffness ellipsoid that is suitable for the task. One derives a formula that makes the manipulator take a posture that provides desired stiffness ellipsoid of the end-point for the task. It follows the simulation study that elucidates the proposed formula successfully working.

References

[1] Shadmehe, R. and Arbib M. A. , A mathematical analysis of the force-stiffness characteristics of muscles in control of a single joint system, Biol. Cybern., Vol.66, 1992, 463-477.

[2] Matthews, P.B.C., The dependence of tension upon extension in the stretch reflex of the soleus muscle of the decerebrated cat, J. of Physiol., Vol. 147, 1959, 521-546.

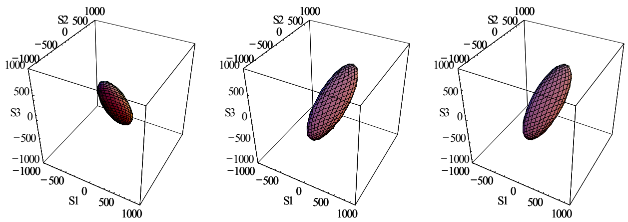

(a) initial (b) desired (c) regulated

Fig.15 Stiffness ellipsoids of the initial posture, desired posture and the regulated posture

frontal view **upper view** **side view**

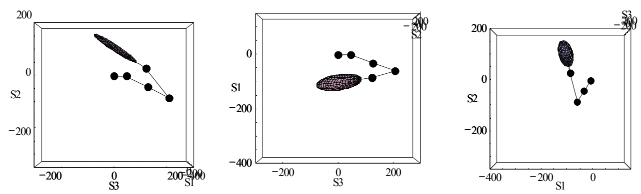

(a) the initial posture and the initial stiffness ellipsoid

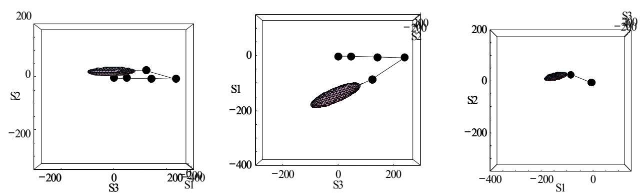

(b) the desired posture and the desired stiffness ellipsoid

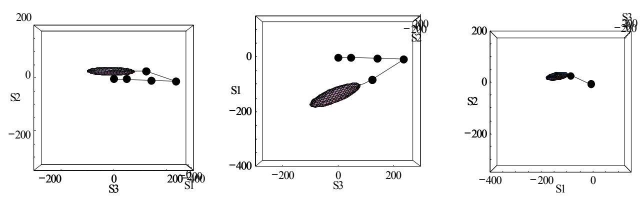

(c) the result of the posture control

Fig.16 Simulation results: the posture and the corresponding stiffness ellipsoid

[3] Fel'dman, A.G., Functional tuning of the neurons system with control of movement or maintenance of a steady posture. Biofizika, *11(3)*, 1966, 498-508.

[4] Hoffer, J.A. and S. Andrearsen. Regulation of soleus muscle stiffness in premammiliary cats, J. of Neurophysiol., *45(2)*, 1981, 267-285.

[5] Dolan, J.M., M.B.Friedman and M.L. Nagurka, "Dynamic and Loaded Impedance of Human Arm Posture," IEEE Trans. on System Man and Cybern., Vol.23, No.3, pp.698/709, 1993.

[6] Mussa-Ivaldi, N. Hogan and E. Bizzi,"Neural, Mechanical and Geometric Factors Subserving Arm Posture in Humans," The Journal of Neuroscience, Vol.5, No.10, pp.2732/2743, 1985.

[7] Jocobsen, S. C., J. E. Wood, D. F. Knutti and K. B. Biggers, " The UTAH/M.I.T. Dextrous Hand: Work in Progress, The Int. Journal of Robotics Res., Vol.3, No.4, pp.21/51, 1984.

[8] Jacobsen, S.C., H. Ko, E. K. Inversen and C.C Davis, "Antagonistic Control of a Tendon Driven Manipulator," Proceedings of the IEEE Int. Conf. on Robotics and Automation, pp. 1334/1339, 1989.

[9] Laurin-Kovitz, K. F., J. E. Colgate and S. D. R. Carnes, "Design of Components for Programmable Passive Impedance," Proceedings of the IEEE Int. Conf. on Robotics and Automation, pp.1476/1481, 1991

[10] Yi, B. J. and Freeman, R. A., "Geometric Characteristics of Antagonistic Stiffness In Redundantly Actuated Mechanisms," Proc. of IEEE Int. Conf. on Robotics & Automation, pp.654/661, 1993.

[11] Kobayasi, H. , Hyoudou, K and Ogane, D. , On Tendon-Driven Robotics Mechanisms with Redundant Tendons, The Int. J. of Robotics Res, 17(15), pp. 561-571, 1998.

[12] Lee, Y.T., H.R. Choi, W. K. Chung and Y. Youm, "Stiffness Control of a Coupled Tendon-Driven Robot Hand," IEEE Control Systems Magazine, pp.10/19,1994.

[13] Yi, B. J. and Freeman, R. A.,"Synthesis of Actively Adjustable Springs by Antagonistic Redundant Actuation," Trans. on ASME, Journal of Dynamic Systems, Measurement and Control, Vol.114, pp.454/461, 1992.

[14] Chen, S. F. and I. Kao,"Conservative Congruence Transformation for Joint and Cartesian Stiffness Matrices of Robotic Hands and Fingers, The Int. J. of Robotics Res., Vol.19, No.9, pp.835/847, 2000.

[15] Koganezawa, K, Y. Shimizu, H. Inomata and T. Nakazawa, "Actuaor with Non-linear Elastic System (ANLES) for Controlling Joint Stiffness of Antagonistic Driving," Proceedings of IEEE International Conference on ROBOTICS AND BIOMIMETICS (ROBIO), Shenyang, China, Aug. 2004,

[16] Koganezawa, K. and Yamazaki, M.,"Mechanical Stiffness Control of Tendon-Driven Joint," Proc. of the 1999 IEEE/RSJ INt. Conf. on Intelligent Robots and Systems, pp.818/825.

[17] Koganezawa, K., Mechanical Stiffness Control for Antagonistically Driven Joints, Proc. of the IEEE/RSJ International Conference on Intelligent Robots & Systems (IROS 2005), Edmonton, Alberta, Canada, 2005.

[18] Koganezawa, K., Toshiki Nakazawa, Tomoya Inaba, "Antagonistic Control of Multi-DOF Joint by Using the Actuator with Non-Linear Elasticity," Proceedings of the 2006 IEEE International Conference on Robotics and Automation, Orlando, Florida - May 2006, pp.2201-2207.